

Rayleigh and Prandtl number scaling in the bulk of Rayleigh-Benard turbulence

Enrico Calzavarini^{1,2}, Detlef Lohse³, Federico Toschi^{2,4}, and Ra'aele Tripiccone^{1,2}¹Dipartimento di Fisica, Università di Ferrara, Via Paradiso 12, I-43100 Ferrara, Italy.²INFN, Via Paradiso 12, I-43100 Ferrara, Italy.³Department of Applied Physics and J. M. Burgers Centre for Fluid Dynamics, University of Twente, 7500 AE Enschede, The Netherlands. and⁴IAC-CNR, Istituto per le Applicazioni del Calcolo, Viale del Policlinico 137, I-00161 Roma, Italy.

(Dated: February 7, 2022)

The Rayleigh and Prandtl number scaling of the Nusselt number Nu , the Reynolds number Re , the temperature fluctuations, and the kinetic and thermal dissipation rates is studied for (numerical) homogeneous Rayleigh-Benard turbulence, i.e., Rayleigh-Benard turbulence with periodic boundary conditions in all directions and a volume forcing of the temperature field by a mean gradient. This system serves as model system for the bulk of Rayleigh-Benard flow and therefore as model for the so called "ultimate regime of thermal convection". With respect to the Rayleigh dependence of Nu and Re we confirm our earlier results [1] which are consistent with the Kraichnan theory [2] and the Grossmann-Lohse (GL) theory [3, 4, 5, 6], which both predict $Nu \propto Ra^{1/2}$ and $Re \propto Ra^{1/2}$. However the Prandtl dependence within these two theories is different. Here we show that the numerical data are consistent with the GL theory $Nu \propto Pr^{1/2}$, $Re \propto Pr^{1/2}$. For the thermal and kinetic dissipation rates we find $\epsilon = (L^2) (Re Pr)^{0.87}$ and $\epsilon_u = (L^4) Re^{2.77}$, also both consistent with the GL theory, whereas the temperature fluctuations do not depend on Ra and Pr . Finally, the dynamics of the heat transport is studied and put into the context of a recent theoretical finding by Doering et al. [7].

I. INTRODUCTION

The scaling of large Rayleigh number (Ra) Rayleigh-Benard convection has attracted tremendous attention in the last two decades [3, 4, 5, 6, 8, 9, 10, 11, 12, 13, 14, 15, 16, 17, 18, 19, 20, 21, 22, 23, 24, 25, 26, 27, 28, 29, 30, 31, 32, 33, 34, 35, 36, 37, 38, 39, 40, 41, 42, 43, 44, 45, 46, 47, 48, 49, 50, 51, 52, 53]. There is increasing agreement that in general there are no clean scaling laws for $Nu(Ra; Pr)$ and $Re(Ra; Pr)$, apart from asymptotic cases. One of these asymptotic cases has been dubbed the "ultimate state of thermal convection" [2], where the heat flux becomes independent of the kinetic viscosity and the thermal diffusivity. The physics of this regime is that the thermal and kinetic boundary layers have broken down or do not play a role any more for the heat flux and the flow is bulk dominated. The original scaling laws suggested for this regime are [2]

$$Nu \propto Ra^{1/2} (\log Ra)^{-3/2} Pr^{1/2} \quad (1)$$

$$Re \propto Ra^{1/2} (\log Ra)^{-1/2} Pr^{1/2}; \quad (2)$$

for $Pr < 0.15$, while for $0.15 < Pr < 1$:

$$Nu \propto Ra^{1/2} (\log Ra)^{-3/2} Pr^{1/4} \quad (3)$$

$$Re \propto Ra^{1/2} (\log Ra)^{-1/2} Pr^{3/4}. \quad (4)$$

The GL theory also gives such an asymptotic regime which is bulk dominated and where the plumes do not play a role [6] (regimes IV_1 and IV_1^0 of Refs. [3, 4, 5, 6]). It has the same Ra dependence as in eqs. (1)–(3), but different Pr dependence, namely

$$Nu \propto Ra^{1/2} Pr^{1/2}; \quad (5)$$

$$Re \propto Ra^{1/2} Pr^{1/2}; \quad (6)$$

As a model of the ultimate regime we had suggested [1] homogeneous RB turbulence, i.e., RB turbulence with periodic boundary conditions in all directions and a volume forcing of the temperature field by a mean gradient [54],

$$\frac{\partial}{\partial t} + (u \cdot \nabla) \theta = \kappa \nabla^2 \theta + \frac{1}{L} u_z; \quad (7)$$

Here $\theta = T + (\Delta L)z$ is the deviation of the temperature from the linear temperature profile $(\Delta L)z$. The velocity field $u(x; t)$ obeys the standard Boussinesq equation,

$$\frac{\partial u}{\partial t} + (u \cdot \nabla) u = -\nabla p + \eta \nabla^2 u + g \hat{z}; \quad (8)$$

Here, α is the thermal expansion coefficient, g gravity, p the pressure, and $\theta(x; t)$ and $u_i(x; t)$ are temperature and velocity field, respectively. Indeed, in Ref. [1] we showed that the numerical results from eqs. (7) and (8) are consistent with the suggested [2, 3, 4, 5, 6] Ra dependence of Nu and Re , $Nu \propto Ra^{1/2}$ and $Re \propto Ra^{1/2}$. However, the Pr dependences of Nu and Re , for which the predictions of Kraichnan [2] and GL [3, 4, 5, 6] are different, has not yet been tested for homogeneous turbulence: this is the first aim of this paper (Section III). Section II contains details of the numerics. In Section IV we study the bulk scaling laws for the thermal and kinetic dissipation rates and compare them with the GL theory. In that Section we study the temperature fluctuations $\theta = \theta^{1/2}$. The dynamics of the flow, including $Nu(t)$

and its PDF (probability density function), is studied in Section V and put into the context of a recent analytical finding by Doering and coworkers [7]. Section VI contains our conclusions.

II. DETAILS OF THE NUMERICS

Our numerical simulation is based on a Lattice Boltzmann Equation (LBE) algorithm on a cubic 240^3 grid. The same scheme and resolution has already been used in [54, 55]. We run two sets of simulations in statistically stationary conditions. The first at fixed $Pr = 1$ varying the Ra number between $9.6 \cdot 10^4$ and $1.4 \cdot 10^5$. The second at fixed $Ra = 1.4 \cdot 10^5$. This, the highest value we can reach at the present resolution, was studied for five different Pr numbers, $1/10, 1/3, 1, 3$ and 4 . We recorded shortly-spaced time series of Nu and root mean squared (rms) values of temperature and velocity and we stored a collection of the whole field configurations, with a coarse time-spacing. The length of each different run ranges between 64 and 166 eddy turnover times. Our simulation was performed on a APEMille machine in a 128 processor configuration [57], [58]. Each eddy turnover times requires on average 4 hours of computation. The total computational time required for the whole set simulations is roughly 150 days. The total number of stored configurations is around 2000.

III. $Nu(Ra; Pr)$ AND $Re(Ra; Pr)$

The Nusselt number is defined as the dimensionless heat flux

$$\begin{aligned} Nu &= \frac{1}{L^{-1}} \langle h_{3T} i_{A,t}(z) \rangle - h_{3T} i_{A,t}(z) \\ &= \frac{\langle h_{3T} i_{A,t}(z) \rangle}{L^{-1}} - 1 \end{aligned} \quad (9)$$

where the average $\langle h_{3T} i_{A,t} \rangle$ is over a horizontal plane and over time. From eqs. (7)–(9) one can derive two exact relations for the volume averaged thermal dissipation rate $\epsilon = \langle \epsilon_i \rangle_V^2$ and the volume averaged kinetic dissipation rate $\epsilon_u = \langle \epsilon_i u_j \rangle_V^2$, namely

$$\epsilon_u = \frac{3}{L^4} Nu Ra Pr^{-2}; \quad (10)$$

$$= \frac{2}{L^2} Nu; \quad (11)$$

One can therefore numerically compute Nu in three different ways: (i) from its direct definition (9), (ii) from the volume averaged kinetic dissipation rate (10), (iii) from the volume averaged thermal dissipation rate (11).

The results are shown in Figure 1a as a function of Ra for $Pr = 1$. There is very good agreement of Nu obtained

from the three different methods for all Ra , giving us further confidence in the convergence of the numerics. If we fit all data points beyond $Ra = 10^5$ with an effective power law, we obtain $Ra \sim Nu^{0.50 \pm 0.05}$, consistent with the asymptotically expected law $Nu \sim Ra^{1/2}$ [59]

In Figure 1b we display Nu as function of Pr for fixed $Ra = 1.4 \cdot 10^5$. For the cases with $Pr \ll 1$ the convergence of the three different methods to calculate Nu is not perfect. This may be due to numerical errors in the resolution of the small scale differences, especially when ϵ and ϵ_u are considerably different. However, one can clearly notice a strong increase of Nu with Pr . A fit with an effective power law gives $Nu \sim Pr^{0.43 \pm 0.07}$, which is consistent with the asymptotic power law $Nu \sim Pr^{1/2}$ suggested by the GL theory and by the small Pr regime (1) suggested by Kraichnan, but not with Kraichnan's large Pr regime (3). Increasing further Pr (at fixed Ra) the flow will eventually laminarize, i.e., can no longer be considered as model system for the bulk of turbulence. This also follows from Figure 2b, in which we show the Reynolds number:

$$Re = \frac{u^0 L}{\nu} \quad (12)$$

as function of Pr for fixed $Ra = 1.4 \cdot 10^5$. Note that this is the fluctuation Reynolds number, defined by the rms velocity fluctuation $u^0 = u'^2^{1/2}$: in homogeneous RB no large scale wind exists. $Re(Pr)$ displays an effective scaling law $Re \sim Pr^{0.55 \pm 0.01}$, consistent with the GL prediction $Pr^{-1/2}$ for the ultimate regime (if one identifies the wind Reynolds number in GL with the fluctuation Reynolds number here) and also with the Kraichnan prediction (1). Also the Ra scaling of Re is consistent with GL (and also with Kraichnan), $Re \sim Ra^{1/2}$, as seen from Figure 2a and as already shown in Ref. [1].

IV. SCALING LAWS FOR ϵ_u , ϵ AND THE TEMPERATURE FLUCTUATIONS

A. Kinetic and thermal dissipations

The homogeneous RB turbulence offers the opportunity to numerically test one of the basic assumptions of the GL theory, namely, that the energy dissipation rate in the bulk scales like

$$\epsilon_{bulk} \sim \frac{3}{L^4} Re^3; \quad (13)$$

In Figure 3(a) we plot $\epsilon_u = (3L^{-4})$ vs. Re for all Ra and Pr and find $\epsilon_u = (3L^{-4}) Re^{2.77 \pm 0.03}$, close to the expectation (13).

The disentanglement of the thermal dissipation rate into two different scaling contributions is less straightforward. The GL theory decomposes:

$$= c_3 (Re Pr)^{1/2} + c_4 (Re Pr); \quad (14)$$

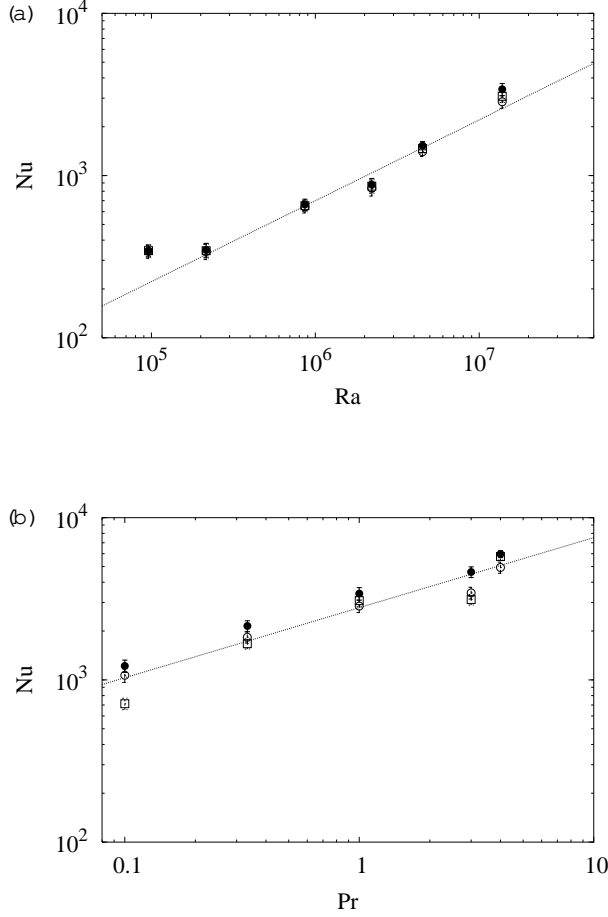


FIG. 1: (a) $Nu(Ra)$ for $Pr = 1$, computed in three different ways: () using Eqn. (8), () using Eqn. (10), and () from Eqn. (11). The power law fits, performed on the mean value of the three different estimates and for $Ra > 10^5$, gives a slope 0.50 ± 0.05 . (b) $Nu(Pr)$ for $Ra = 1.4 \cdot 10^7$, fit performed as before, with a resulting slope of 0.43 ± 0.07 .

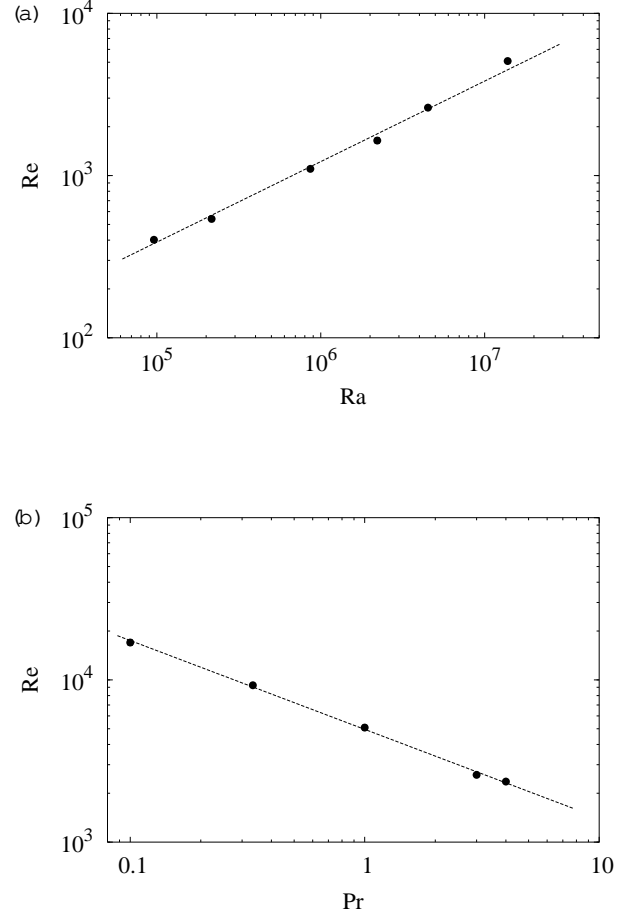


FIG. 2: (a) $Re(Ra)$ for $Pr = 1$, with a fitted slope 0.50 ± 0.02 . (b) $Re(Pr)$ for $Ra = 1.4 \cdot 10^7$, with a fitted slope 0.55 ± 0.01 .

where the first term has been interpreted as boundary layer and plume contribution ν_{pl} and the second one as background contribution ν_{bg} [6]. The prefactors c_3 and c_4 are given in Ref.[4]. Plumes are interpreted as detached boundary layer [6]. For homogeneous RB turbulence one would expect the background contributions to be dominant as there is no boundary layer. But still some plumes may also develop in the bulk and this is confirmed by the fact that we find a scaling law in between the asymptotes $(RePr)^{1/2}$ and $RePr$, namely, $(RePr)^{0.87 \pm 0.04}$: closer to the background behavior just as one would guess.

B. Temperature fluctuations

In our numerics we find the temperature fluctuations $\theta = \theta' / \theta_0$ to be independent from Ra and Pr , see Figure 4. That figure shows that we have $\theta' = 0$ for all Ra and Pr within our numerical precision. In contrast, Ref. [6] predicted a dependence of the thermal fluctuations on both Ra and Pr , namely $\theta = (PrRa)^{-1/8}$ for the regimes IV_1 and IV_1^0 which correspond to the bulk of turbulence analysed here. Our interpretation of Figure 4 is that the bulk turbulence only has one temperature scale, namely θ . For real RB turbulence it is the boundary layer dynamics which introduces further temperature scales, leading to the Ra and Pr number dependence of the temperature fluctuations observed in experiments [8, 19, 50, 51].

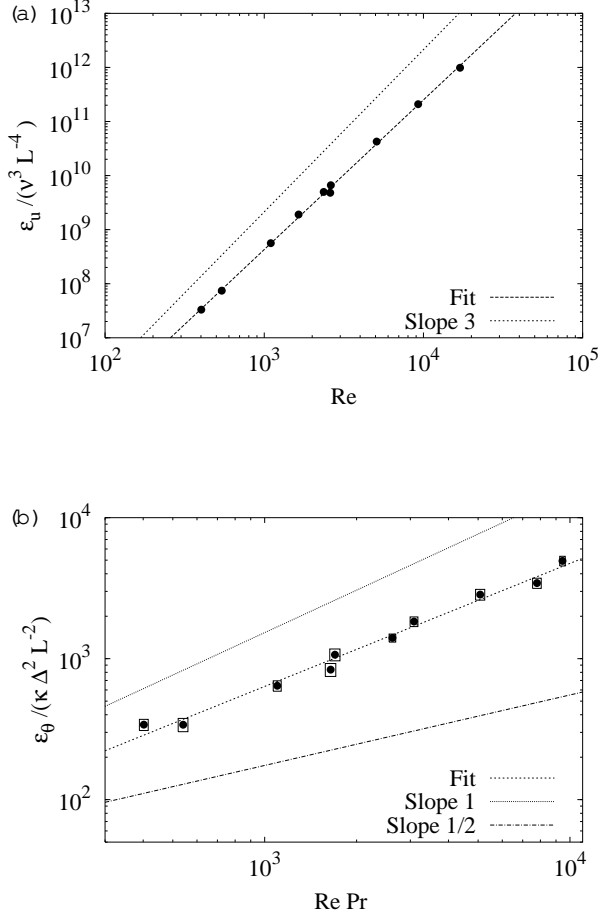


FIG. 3: (a) We show $\varepsilon_u = (\nu^3 L^{-4})$ vs. Re . The fit gives a slope of 2.77 ± 0.03 , slope 3 is shown for comparison. (b) $\varepsilon_\theta = (\kappa^2 L^{-2})$ vs. $Re Pr$. We obtained a fitted slope 0.87 ± 0.04 while slopes 1 and $1/2$ are also shown for comparison.

V. DYNAMICS OF THE FLOW

In this section we provide an insight into the dynamics of the periodic Rayleigh-Benard flow. A bidimensional vertical snapshot of the flow is shown in Figure 5. Already from this pictorial view the presence of an upward moving hot column and a downward moving cold column is clearly evident.

Indeed these large scale structure can be related to the presence of "elevators modes" (or jets, forming in the flow) growing in time until finally breaking down due to some instability mechanisms.

As proposed by Doering and collaborators in [7] it is possible to predict the presence of these modes directly starting from equations (7) and (8). Doering et al. showed that, due to the periodic boundary conditions, this coupled system of equations admits a particular solution $\theta = \theta_0 e^{-t} \sin(k_x x)$, $u = u_0 e^{-t} \sin(k_x x)$,

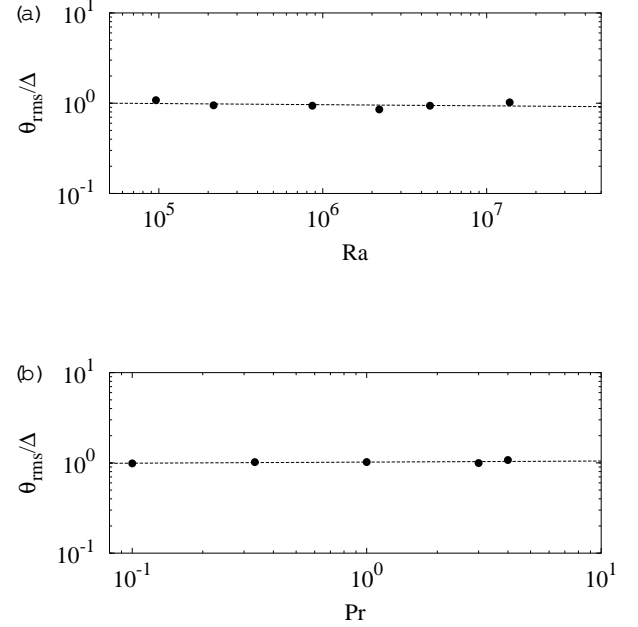


FIG. 4: (a) Normalized temperature variance $\theta_{rms} = \theta_rms / \Delta$ vs. Ra at fixed $Pr = 1$. (b) $\theta_{rms} = \theta_rms / \Delta$ vs. Pr at fixed $Ra = 1.4 \times 10^7$.

$u_2 = u_1 = 0$, which is independent from the vertical coordinate z (here $k = (k_x; k_y)$) and with:

$$= \frac{1}{2} (Pr + 1) k^2 + \frac{1}{2} (Pr + 1)^2 k^4 + 4Pr \frac{Ra}{L^4} k^4 \quad (15)$$

From equation (15) one finds that the first unstable mode appears for $Ra = Ra_c = (2)^4 = 1558.54$, corresponding to the instability of the smallest possible wavenumber in the system, i.e. $k^2 = (2\pi/L)^2 n^2$ with $n = (1; 0)$.

The presence of accelerating modes with growth rate controlled by γ can also be seen from Figure 6 where we show $Nu(t)$ on log-scale (notice the huge range over which Nu fluctuates).

In Figure 7 we show the PDF of $Nu(t)$ which is strongly skewed towards large Nu values. This asymmetry reflects the periods of exponential growth (also visible in Figure 6). As can be seen in Figure 8, for all Ra and Pr the system typically spends 54% of the time in growing modes.

Also the relative fluctuations of Nu on the Ra and Pr numbers (see Figure 9) seems to indicate no dependencies, at least in the range of parameters studied.

Despite the presence of exact exploding solutions, our system clearly shows that in the turbulent regime these

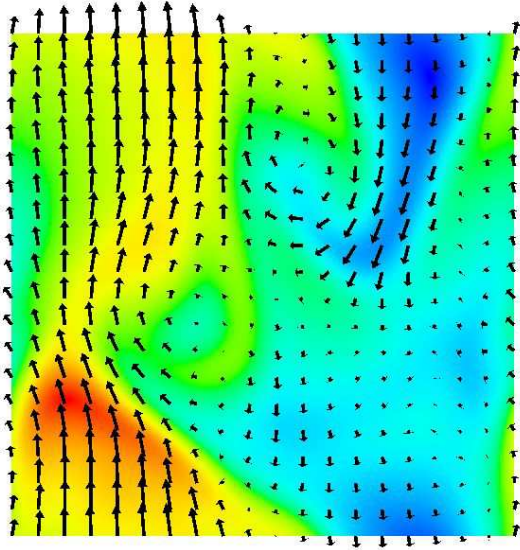


FIG. 5: Snapshot of the flow, showing elevator modes and jets. Here is shown in colors: red and yellow encode for positive values, with red greater in amplitude than yellow, green is for small values around zero, while blue stands for the negative values, the dark blue stands for the more negative values. Velocity in the same plane is shown with arrows.

solutions become unstable due to some yet to be explored instability mechanism. The interplay between exploding modes and destabilization sets the value of the Nusselt number, i.e. the heat transfer through the cell.

We stress that the study of the dynamics of the explosive solutions and of their successive collapses in a turbulent cell is crucial for the understanding the behaviour of "integral" quantities, like, for example, the heat transfer.

VI. CONCLUSIONS

In conclusion, we confirmed that both the Ra - and the Pr -scaling of Nu and Re in homogeneous Rayleigh-Bénard convection is consistent with the suggested scaling laws of the Grossmann-Lohse theory for the bulk-dominated regime (regime IV_1 of [3, 4, 5]), which is the so-called "ultimate regime of thermal convection". We also showed that the thermal and kinetic dissipations scale roughly as assumed in that theory. The temperature fluctuations do not show any Ra or Pr dependence for homogeneous Rayleigh-Bénard convection. From the dynamics the heat transport and flow visualizations we identify "elevator modes" which are brought into the context of a recent analytical finding by Doering et al. In future work we plan to further elucidate the flow organization and in particular the instability mechanisms of the elevator modes which set the Nusselt number in homogeneous RB flow and therefore presumably also in the

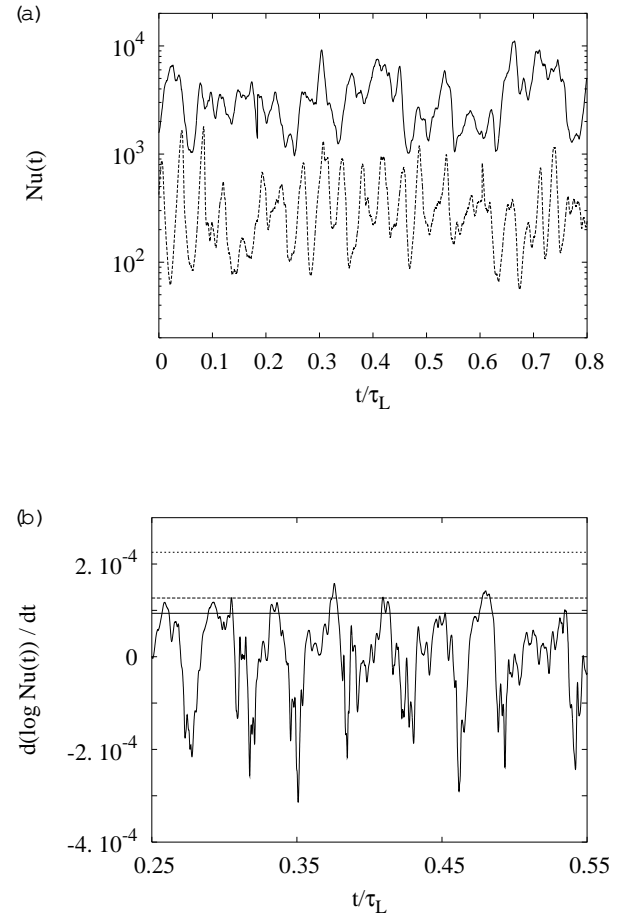


FIG. 6: (a) Time series $Nu(t)$ for $Ra = 1.4 \cdot 10^6$ (top) and $Ra = 9.6 \cdot 10^6$ (bottom), in both cases $Pr = 1$. (b) Logarithmic derivative of $Nu(t)$ for $Ra = 9.6 \cdot 10^6$, here reproduced only for a small time section of the data in (a). The series of horizontal lines represent the exponential rate of growing respectively (top to bottom) for the mode $(0;1)$, $(0;2)$, and $(1;2)$.

ultimate regime of thermal convection.

Acknowledgments

We thank Charlie Doering for stimulating discussions on section V. D.L. wishes to thank Siegfried Grossmann for extensive discussions and exchange over the years. This work is part of the research programme of the Stichting voor Fundamenteel Onderzoek der Materie (FOM), which is financially supported by the Nederlandse Organisatie voor Wetenschappelijk Onderzoek (NWO). Support by the European Union under contract HPRN-CT-2000-00162 "Non Ideal Turbulence" is also acknowledged. This research was also supported by the INFN, through access to the APEMille computer resources. E.C. has

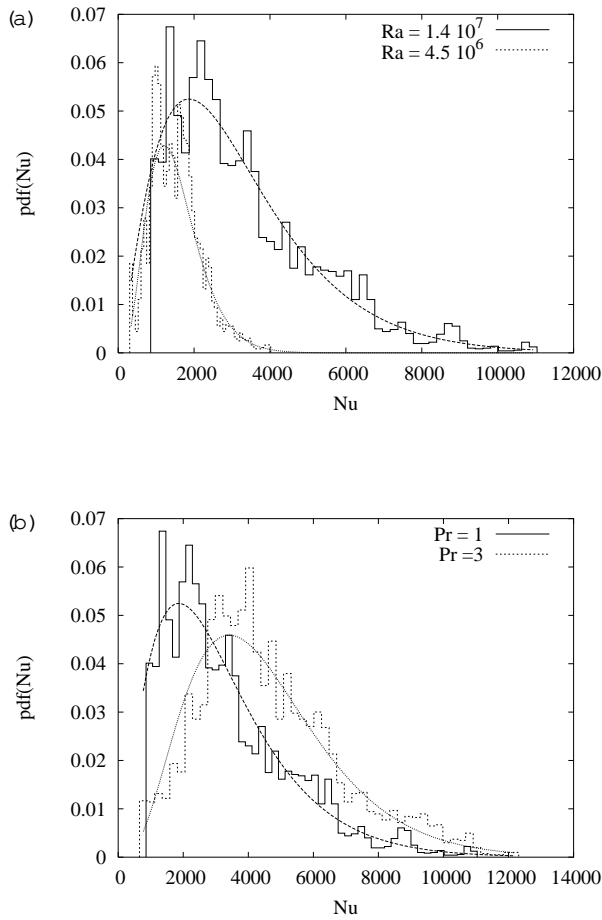


FIG. 7: (a) and (b): PDF of $Nu(t)$ for different Ra and Pr . The superimposed curves correspond to a two parameter Gamma distribution $t, Nu^a \exp(-bNu)$ [56].

been supported by Neuricam spa (Trento, Italy) in the framework of a doctoral grant program with the University of Ferrara and during his visit at University of Twente by SARA through the HPC-Europe program.

-
- [1] D. Lohse and F. Toschi, The ultimate state of thermal convection, *Phys. Rev. Lett.* 90, 034502 (2003).
 - [2] R. H. Kraichnan, Turbulent thermal convection at arbitrary Prandtl number, *Phys. Fluids* 5, 1374 (1962).
 - [3] S. Grossmann and D. Lohse, Scaling in thermal convection: A unifying view, *J. Fluid Mech.* 407, 27 (2000).
 - [4] S. Grossmann and D. Lohse, Thermal convection for large Prandtl number, *Phys. Rev. Lett.* 86, 3316 (2001).
 - [5] S. Grossmann and D. Lohse, Prandtl and Rayleigh number dependence of the Reynolds number in turbulent thermal convection, *Phys. Rev. E* 66, 016305 (2002).
 - [6] S. Grossmann and D. Lohse, Fluctuations in turbulent Rayleigh-Benard convection: The role of plumes, *Phys. Fluids* 16, December (2004).
 - [7] C. R. Doering, J. D. Gibbon, and A. Tanabe, Comment on ultimate state of thermal convection, *Phys. Rev. Lett.* x, y (2005).
 - [8] B. Castaing, G. Gunaratne, F. Heslot, L. Kadano, A. Libchaber, S. Thomae, X. Z. Wu, S. Zaleski, and G. Zanetti, Scaling of hard thermal turbulence in Rayleigh-Benard convection, *J. Fluid Mech.* 204, 1 (1989).
 - [9] X. Z. Wu, L. Kadano, A. Libchaber, and M. Sano, Frequency power spectrum of temperature fluctuation in free convection, *Phys. Rev. Lett.* 64, 2140 (1990).
 - [10] X. Z. Wu and A. Libchaber, Scaling relations in thermal turbulence: The aspect ratio dependence, *Phys. Rev. A* 45, 842 (1992).
 - [11] G. Zocchi, E. Moses, and A. Libchaber, Coherent structures in turbulent convection: an experimental study, *Physica A* 166, 387 (1990).
 - [12] A. Belmonte, A. Tilgner, and A. Libchaber, Boundary layer length scales in thermal turbulence, *Phys. Rev. Lett.* 70, 4067 (1993).
 - [13] L. P. Kadano, Turbulent heat flow: Structures and scaling, *Phys. Today* 54, 34 (2001).
 - [14] X. Chavanne, F. Chilla, B. Castaing, B. Hebral, B.

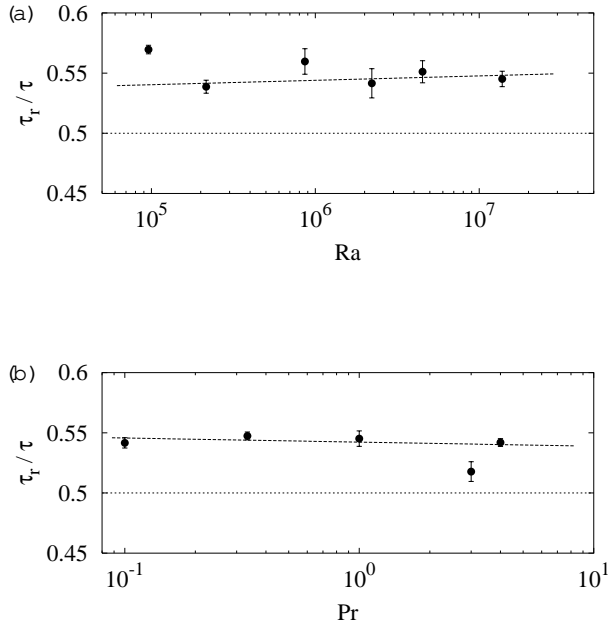


FIG. 8: Normalized rising time τ_r as a function of (a) Ra for $Pr = 1$ and (b) Pr for $Ra = 1.4 \times 10^5$. The time τ_r is the total time with positive slope of $Nu(t)$, whereas the time τ is the total time of the run. The slope of the two fits in the shown graphs is compatible with zero, the overall mean value for τ_r is 0.54.

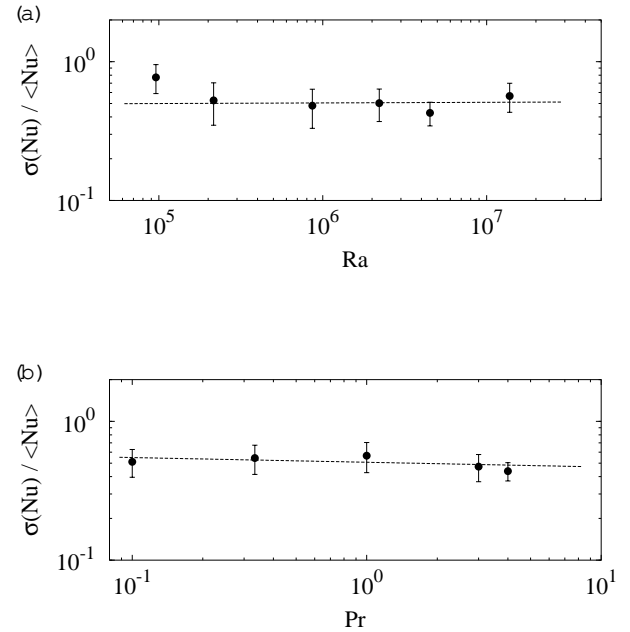


FIG. 9: Relative fluctuations $\sigma(Nu) / \langle Nu \rangle$, where $\sigma(Nu) = \sqrt{\langle Nu(t)^2 \rangle - \langle Nu(t) \rangle^2}$, as function of (a) Ra for $Pr = 1$ and (b) Pr for $Ra = 1.4 \times 10^5$.

- Chabaud, and J. Chaussy, Observation of the ultimate regime in Rayleigh-Benard convection, *Phys. Rev. Lett.* 79, 3648 (1997).
- [15] X. Chavanne, F. Chilla, B. Chabaud, B. Castaing, and B. Hebral, Turbulent Rayleigh-Benard convection in gaseous and liquid He, *Phys. Fluids* 13, 1300 (2001).
- [16] P. E. Roche, B. Castaing, B. Chabaud, and B. Hebral, Observation of the $1/2$ power law in Rayleigh-Benard convection, *Phys. Rev. E* 63, 045303 (2001).
- [17] P. E. Roche, B. Castaing, B. Chabaud, and B. Hebral, Prandtl and Rayleigh numbers dependences in Rayleigh-Benard convection, *Europhys. Lett.* 58, 693 (2002).
- [18] E. D. Siggia, High Rayleigh number convection, *Annu. Rev. Fluid Mech.* 26, 137 (1994).
- [19] J. Niemela, L. Skrbek, K. R. Sreenivasan, and R. Donnelly, Turbulent convection at very high Rayleigh numbers, *Nature* 404, 837 (2000).
- [20] J. Niemela, L. Skrbek, K. R. Sreenivasan, and R. J. Donnelly, The wind in confined thermal turbulence, *J. Fluid Mech.* 449, 169 (2001).
- [21] J. Niemela and K. R. Sreenivasan, Confined turbulent convection, *J. Fluid Mech.* 481, 355 (2003).
- [22] S. Grossmann and D. Lohse, On geometry effects in Rayleigh-Benard convection, *J. Fluid Mech.* 486, 105 (2003).
- [23] X. Xu, K. M. S. Bajaj, and G. Ahlers, Heat transport in turbulent Rayleigh-Benard convection, *Phys. Rev. Lett.* 84, 4357 (2000).
- [24] G. Ahlers and X. Xu, Prandtl-number dependence of heat transport in turbulent Rayleigh-Benard convection, *Phys. Rev. Lett.* 86, 3320 (2001).
- [25] A. Nikolaenko and G. Ahlers, Nusselt number measurements for turbulent Rayleigh-Benard convection, *Phys. Rev. Lett.* 91, 084501 (2003).
- [26] R. Verzicco and R. Camussi, Prandtl number effects in convective turbulence, *J. Fluid Mech.* 383, 55 (1999).
- [27] R. Verzicco, Turbulent thermal convection in a closed domain: viscous boundary layer and mean flow effects, *Eur. Phys. J. B* 35, 133 (2003).
- [28] R. Verzicco and R. Camussi, Numerical experiments on strongly turbulent thermal convection in a slender cylindrical cell, *J. Fluid Mech.* 477, 19 (2003).
- [29] R. Camussi and R. Verzicco, Convective turbulence in mercury: Scaling laws and spectra, *Phys. Fluids* 10, 516 (1999).
- [30] X. D. Shang, X. L. Qiu, P. Tong, and K. Q. Xia, Measured local heat transport in turbulent Rayleigh-Benard convection, *Phys. Rev. Lett.* 90, 074501 (2003).
- [31] Y. B. Du and P. Tong, Enhanced heat transport in turbulent convection over a rough surface, *Phys. Rev. Lett.* 81, 987 (1998).
- [32] Y. Shen, P. Tong, and K. Q. Xia, Turbulent convection over rough surfaces, *Phys. Rev. Lett.* 76, 908 (1996).
- [33] Y. B. Du and P. Tong, Turbulent thermal convection in a cell with ordered rough boundaries, *J. Fluid Mech.* 407, 57 (2000).
- [34] X. L. Qiu and P. Tong, Onset of coherent oscillations in turbulent Rayleigh-Benard convection, *Phys. Rev. Lett.*

- 87, 094501 (2001).
- [35] S. Cioni, S. Ciliberto, and J. Sommeria, Strongly turbulent Rayleigh-Benard convection in mercury: comparison with results at moderate Prandtl number, *J. Fluid Mech.* 335, 111 (1997).
 - [36] S. Ciliberto and C. Laroche, Random roughness of boundary increases the turbulent convection scaling exponent, *Phys. Rev. Lett.* 82, 3998 (1999).
 - [37] K.-Q. Xia and S.-L. Lui, Turbulent thermal convection with an obstructed sidewall, *Phys. Rev. Lett.* 79, 5006 (1997).
 - [38] K.-Q. Xia, S. Lam, and S. Q. Zhou, Heat-ux measurement in high-Prandtl-number turbulent Rayleigh-Benard convection, *Phys. Rev. Lett.* 88, 064501 (2002).
 - [39] S. Lam, X. D. Shang, S. Q. Zhou, and K. Q. Xia, Prandtl-number dependence of the viscous boundary layer and the Reynolds-number in Rayleigh-Benard convection, *Phys. Rev. E* 65, 066306 (2002).
 - [40] H. D. Xi, S. Lam, and K. Q. Xia, From laminar plumes to organized flows: the onset of large-scale circulation in turbulent thermal convection, *J. Fluid Mech.* 503, 47 (2004).
 - [41] E. S. C. Ching, Heat-ux and shear rate in turbulent convection, *Phys. Rev. E* 55, 1189 (1997).
 - [42] E. S. C. Ching and K. F. Lo, Heat transport by uid flows with prescribed velocity fields, *Phys. Rev. E* 64, 046302 (2001).
 - [43] E. S. C. Ching and K. M. Pang, Dependence of heat transport on the strength and shear rate of circulating flows, *Eur. Phys. J. B* 27, 559 (2002).
 - [44] T. Takeshita, T. Segawa, J. A. Glazier, and M. Sano, Thermal turbulence in mercury, *Phys. Rev. Lett.* 76, 1465 (1996).
 - [45] A. Naert, T. Segawa, and M. Sano, High-Reynolds-number thermal turbulence in mercury, *Phys. Rev. E* 56, R1302 (1997).
 - [46] T. Segawa, A. Naert, and M. Sano, Matched boundary layers in turbulent Rayleigh-Benard convection of mercury, *Phys. Rev. E* 57, 557 (1998).
 - [47] J. Sommeria, The elusive ultimate state of thermal convection, *Nature* 398, 294 (1999).
 - [48] J. A. Glazier, T. Segawa, A. Naert, and M. Sano, Evidence against ultrahard thermal turbulence at very high Rayleigh numbers, *Nature* 398, 307 (1999).
 - [49] C. Doering and P. Constantin, Variational bounds on energy dissipation in incompressible flows: III. Convection, *Phys. Rev. E* 53, 5957 (1996).
 - [50] Z. A. Daza and R. E. Ecke, Does turbulent convection feel the shape of the container?, *Phys. Rev. Lett.* 87, 184501 (2001).
 - [51] Z. A. Daza and R. E. Ecke, Prandtl-number dependence of interior temperature and velocity fluctuations in turbulent convection, *Phys. Rev. E* 66, 045301 (2002).
 - [52] S. Kenjeres and K. Hanjalic, Numerical insight into flow structure in ultraturbulent thermal convection, *Phys. Rev. E* 66, 036307 (2002).
 - [53] M. Breuer, S. Wessling, J. Schmalz, and U. Hansen, Effect of inertia in Rayleigh-Benard convection, *Phys. Rev. E* 69, 026302 (2004).
 - [54] L. Biferale, E. Calzavarini, F. Toschi, and R. Tripiccone, Universality of anisotropic fluctuations from numerical simulations of turbulent flows, *Europhys. Lett.* 64, 461 (2003).
 - [55] E. Calzavarini, F. Toschi, and R. Tripiccone, Evidences of Bolgiano-Obukhov scaling in three-dimensional Rayleigh-Benard convection, *Phys. Rev. E* 66, 016304 (2002).
 - [56] S. Aumaitre and S. Fauve, Statistical properties of fluctuations of the heat transfer in turbulent convection, *Europhys. Lett.* 62, 822 (2003).
 - [57] R. Tripiccone, APEmille, *Parall. Comp.* 25 (10-11), 1297 (1999).
 - [58] A. Bartoloni et al., Status of APEmille, *Nucl. Phys. B* 106, 1043 (2002).
 - [59] In our previous paper [1] the overall magnitude of Nu was affected by a normalization error, hence all points of Fig. (1) of that paper should be multiplied by a factor 240 (corresponding to the grid size of our simulation). This of course does not affect the scaling exponent given there.